JOURNAL OF MATERIALS SCIENCE **37** (2002) 2293–2303

Crystallization of leucite as the main phase in glass doped with fluorine anions

M. B. TOŠIĆ
Institute for Technology of Nuclear and other Mineral Raw Materials, 86 Franchet d Esperey, 11000 Belgrade, Yugoslavia
E-mail: m.tosic@itnms.ac.yu

R. Ž. DIMITRIJEVIĆ
Faculty of Mining and Geology, University of Belgrade, 7 Djušina, 11000 Belgrade, Yugoslavia

M. M. MITROVIĆ
Faculty of Physics, University of Belgrade, 12-16 Studentski Trg, 11000 Belgrade, Yugoslavia

The crystallization of a multicomponent glass containing 1.63 wt% of F^- anions was studied. The results show in powder glass with particle sizes less than 0.15 mm, that surface crystallization is dominant, whereby two phases: leucite and dioside are formed. In glass powder or particle size about 0.15 mm, three phases, phlogopite, diopside and leucite, are formed, accompanied by an abrupt decrease in the resistance of the glass to crystallization. If the particle sizes are in the range 0.15 to 0.45 mm, both surface and volume crystallization are significant, while with particle sizes >0.45 mm, volume crystallization is dominant. Two nucleation temperatures, $T_{n1} = 655^\circ$C and $T_{n2} = 675^\circ$C, were determined in the temperature range of 600–710°C. These temperatures satisfy the condition that $T_n \geq T_g$. Crystallization of bulk glass occurs in the temperature range of $T_c = 870$–1100°C, the crystal phases appearing in the sequence: phlogopite, followed by diopside, followed by leucite. Kinetical and microstructural studies show that the crystallization process is controlled by volume diffusion.

1. Introduction

Glass crystallization opens a wide range of possibilities for modeling specific properties of new glass-ceramic materials. From the structural point of view, a high grade glass-ceramic demands a fine-grained microstructure, developing in the glass at a high nucleus density. This can be achieved by homogenous nucleation, which occurs in many silicate systems when subjected to large undercoolings [1, 2]. Despite considerable advancement in the comprehension of nucleation in glasses, many questions remain unanswered. For example, homogenous and heterogeneous nucleation in glasses are still insufficiently distinguishable [2]. This is partly due to the fact that, according to the available reports, homogenous nucleation has been investigated primarily in glasses of relatively simple composition.

The studies performed so far prove that the use of selective nucleating agents, whose effect on the crystallization process is complex, is an efficient way to obtain fine-grained microstructure [3]. Their influence is attributed to the activity of the ions introduced into the glass. In this sense, oxygen-fluorine anionic substitution is interesting. Since the radii of the oxygen ion and fluorine ion are similar, some of the oxygen ions can be substituted by fluorine in almost all oxide glasses. Fluorine, appearing in a single-valent oxide state, does not have a net developing effect when it replaces oxygen in glass, lowering the viscosity of the melt in that way. Consequently, all processes proceeding in a glass at a slow rate, due to the high melt viscosity, become accelerated after fluorine addition. Phase separation, as a primary glass crystallization process, is of particular significance. Hence, oxygen-fluorine anionic substitution considerably increases the tendency of phase separation in a glass also indirectly influencing the formation of nuclei [3].

The study presented in this paper is a continuation of studies on the crystallization of glasses based on the complex system SiO_2-Al_2O_3-CaO-MgO-K_2O, with the separation of the framework pseudotetragonal aluminosilicate leucite ($KAlSi_2O_6$) as the main crystal phase [4]. The structure of leucite and its interesting reversible phase transformation make it convenient for certain applications [5, 6]. Due to this, the phase formation of leucite is the subject of constant interest.

The starting composition was as follows: 50.5 $SiO_2 \cdot 18.5Al_2O_3 \cdot 10.5CaO \cdot 10.5MgO \cdot 10K_2O$ (wt%). CaF_2 was added to this composition in the amount necessary to bring the content of F^- anions to 1.5 wt%. The aim of this study, performed under both isothermal

and non-isothermal conditions, was to investigate in detail the crystallization of this glass.

2. Experimental

The glass was prepared with reagent grade Al_2O_3, MgO, CaO, CaF_2 and K_2CO_3, and highpurity quartz (>99.5% SiO_2). Premixed powder was melted in an electric furnance, in a platinum crucible for $t = 60$ mins at $T = 1500°C$. The glass samples were transparent, without visible residual gas bubbles.

The first series of experiments was performed under non-isothermal conditions, using a Netzch STA 409 EP device, using Al_2O_3 powder as the reference material.

In order to determine the dominant crystallization mechanism, powder samples of the following granulations were prepared: <0.038; 0.038–0.050; 0.050–0.1; 0.1–0.2; 0.2–0.3; 0.3–0.4; 0.4–0.5; 0.5–0.63; 0.63–0.8 and 0.8–1.0 mm. In the experiments, a constant weight (100 mg) of the samples was heated at a heating rate $v = 5°C/min$.

The nucleation process was studied using powder samples with 0.5–0.63 mm granulation. The samples were heated at a rate of 7.5°C/min up to the temperatures $T = 600$, 640, 650, 655, 660, 665, 670, 675, 680, 685, 690, 700 and 710°C, and kept at these temperatures for $t = 180$ min; after that, heating was continued at the same rate to $T = 1100°C$.

In order to determine the kinetic parameters of crystallization, experiments were performed with granulations <0.038 mm and 0.5–0.63 mm. The samples were investigated at heating rates: $v = 2.5$, 4, 5, 6, 7.5 and 10°C/min.

A second series of experiments was performed with bulk samples, under isothermal conditions, in a two-stage regime. The experiments were performed in an electric furnace with automatic regulation and a temperature accuracy in the range of ±2°C. The samples were first treated isothermally at the nucleation temperatures $T_{n1} = 655°C$, i.e. $T_{n2} = 675°C$ for $t_n = 600$ min, followed by further heating at a rate of $v = 2°C/min$ until the crystallization temperature was reached. The crystallization temperatures were in the range $T_c = 870$–1100°C. The samples were kept at the crystallization temperatures for different times, in the range $t_c = 15$–600 mins. The treated samples were then exposed to X-ray powder diffraction (XRD) and microscopic analyses.

Dilatometric measurings were carried out on samples 3 mm in diameter, 40 mm long. The samples were heated at a rate $v = 10°C/min$, in the temperature range $T = 20$–820°C. Before measuring, the samples were kept at $T = 700°C$ for $t = 30$ min.

The phase composition of the investigated samples was determined by the XRD method. The powder patterns were obtained on a Philips PW-1710 automated diffractometer using the experimental conditions described elsewhere [4]. The quantitative amount of crystalline phase in the glass-ceramics were determined using the full profile matching mode of the Rietveld refinement technique [7], using the Fullproof programme [8]. Published structural data for the determined minerals were used as the starting parameters of the initial refinement.

Investigation of crystal morphology was carried out by scanning electron microscopy using a Jeol JSM 840 A microscope. The samples were gold sputtered in a Jeol JFC 1100 ion sputter.

3. Results and discussion

3.1. The chemical composition of glass

The results of chemical analyses show that the composition of the obtained glass was as follows (in wt%): $50.7SiO_2 \cdot 18.10Al_2O_3 \cdot 7.46CaO \cdot 3.35CaF_2 \cdot 10.27 MgO \cdot 0.13Na_2O \cdot 9.34K_2O$. The content of F^- anions in the glass was 1.63 wt%. Such a content of F^- anions was expected to produce detectable changes of the crystallization kinetics and mechanism of the glass. The composition of this glass does not conform to the leucite stoichiometric composition.

3.2. Crystallization of powder glass

Previous investigations of crystallization in glasses showed that the particle size of the powder glass has an influence on the mechanism of its crystallization [9]. Surface and volume crystallization mechanisms compete in the same glass, one usually being dominant. For assessment of the surface and bulk crystallization, the method proposed by Ray *et al.* [10] is suggested. According to this method, the parameters (δT_p) and $T_p^2/(\Delta T)_p$ are plotted as a function of particle size, where δT_p is the maximum height of the DTA peak. T_p is the temperature of the peak and $(\delta T)_p$ is the width at half the peak maximum. These parameters depend on the specific mechanism of crystallization. δT_p is proportional to the number of nuclei contained in the glass [11] and $T_p^2/(\Delta T)_p$ is related to the crystal growth dimension, according to the following relation [12]

$$n = \frac{2.5 \cdot R}{E_a} \cdot \frac{T_p^2}{(\Delta T)_p} \tag{1}$$

where R is the gas constant, E_a is the activation energy of crystal growth and n the Avrami parameter. If E_a does not depend on the particle size and temperature (at least in the temperature range of the DTA experiment), the relationship between $T_p^2/(\Delta T)_p$ and particle size can be used as a qualitative measure of the surface and volume crystallization.

The DTA curves recorded at a heating rate $v = 5°C/min$ on samples the particle sizes of which were <0.038 mm to 1 mm illustrate three different behaviours of the oxothermic peaks. For particle sizes <0.038 mm to 0.1 mm, a wide exothermic peak appears in the temperature range $T_p = 989.4$–1006.1°C. For particle sizes between 0.1–0.2 mm, two successive exothermic peaks appear: a higher temperature peak at $T_{p1} = 962.9°C$ and a lower one at $T_{p2} = 1007.6°C$. Finally, for particle sizes between 0.2 mm to 1.0 mm, a high, narrow exothermic peak appears in the temperature range $T_p = 960.9$–977°C. The DTA curves recorded with samples of particle sizes <0.038 mm, 0.1–0.2 mm and 0.63–0.8 mm, which illustrate such behaviour, are presented in Fig. 1.

The dependence of the peak crystallization temperature (T_p) on the average particle size is

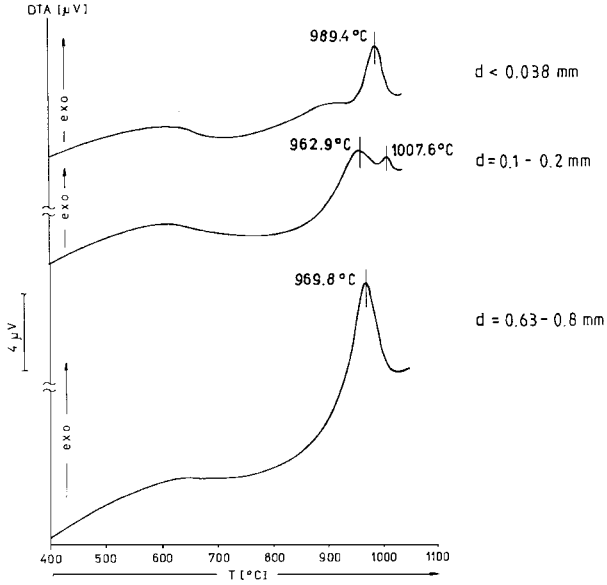

Figure 1 DTA traces recorded for powder samples particle size <0.038 mm, 0.1–0.2 mm and 0.63–0.8 mm, at heating rate 5°C/min and sample weight, 100 mg.

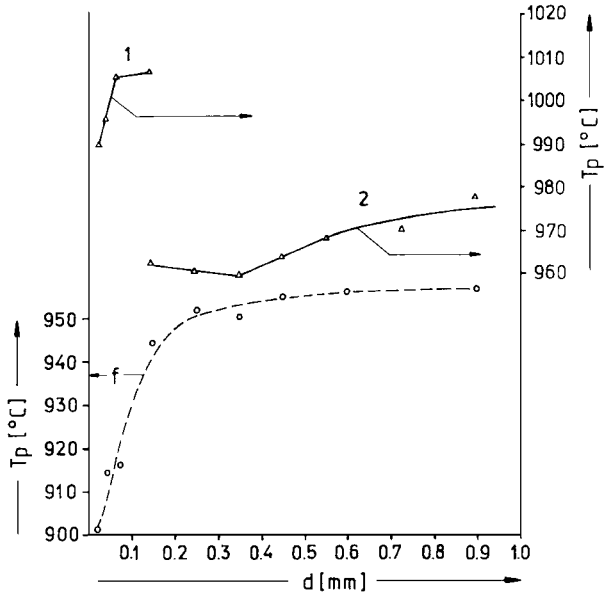

Figure 2 T_p as a function of particle size for glass containing 1.63 wt% of the F^- anions (curves 1 and 2) and glass containing 0.77 wt% of the F^- anions [4] (curve f).

presented in Fig. 2 (curves 1 and 2). For comparison, the f curve referring to the glass of the same composition, but also containing 0.77 wt% of F^- anions is also presented [4]. As can be seen from Fig. 2, increasing the F^- anion content to 1.63 wt% caused a drastic change in T_p behaviour. With this glass, T_p first increases with increasing particle size till the average size reaches 0.15 mm (curve 1), then decreases and finally increases again (curve 2). In order to understand such behaviour, it is necessary to identify the crystal phases formed under such conditions. For this reason, additional experiments were performed in which the samples were heated at a rate $v = 5$°C/min until the temperature of the crystallization peaks was reached and then kept at these temperatures for $t = 15$ min. XRD patterns of these samples are presented in Fig. 3. They show that samples with granulations <0.038 mm

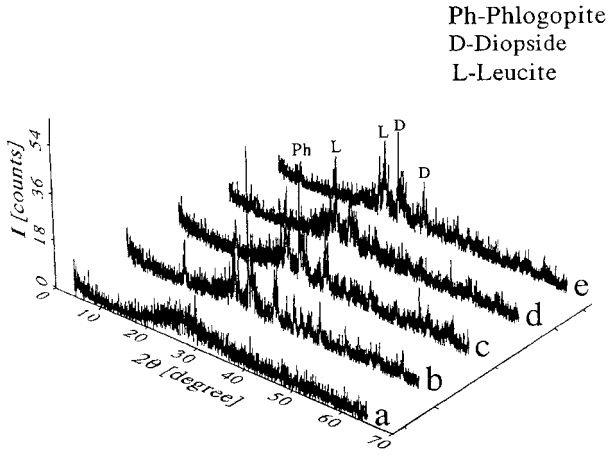

Figure 3 XRD patterns of (a) initial glass and powder samples particle size: (b) <0.038 mm, annealed at $T_c = 990$°C, (c) 0.05–0.1 mm, annealed at $T_c = 1006$°C, (d) 0.1–0.2 mm, annealed at $T_c = 963$° and (e) 0.63–0.8 mm, annealed at $T_c = 970$°C.

and 0.05–0.1 mm consist of leucite and diopside. However, samples with granulations of 0.1–0.2 mm and 0.63–0.8 mm are characterized by the appearance of phlogopite, diopside and leucite phases. According to these results, it can be concluded that for samples of average particle sizes <0.15 mm, leucite and diopside phases are formed, with crystallization peaks occurring in the higher temperature range. When the particle size reaches about 0.15 mm, the formation of the phlogopite phase is also initiated: so, for samples of average particle size >0.15 mm, all three phases, leucite, diopside and phlogopite, are present, with crystallization peaks occurring in the lower temperature range.

These results suggest that the appearance of the phlogopite phase is connected to the glass crystallization mechanism. With the smallest particle sizes, surface nuclei are dominant. Of the total number of nuclei, the number of phlogopite nuclei is negligible because of the low content of F^- anions in the very small bulk volume of the particles. For this reason, probably, the formation of the phlogopite phase was not identified, but only the formation of the leucite and diopside phases. With increasing particle size, a relative number of surface nuclei decreases, with the consequent increase of the crystallization peak temperature and the resistance of the glass to crystallization (curve 1). Such a behaviour is in agreement with curve f corresponding to a glass with a lower content of F^- anions (0.77 wt%), where only leucite and diopside phases are formed. Therefore, when the average particle size is <0.15 mm, and the F^- anion content is 1.63 wt%, the influence of fluorine on the crystallization properties of the glass is not detectable. When the particle sizes are in the range of 0.1–0.2 mm, the behaviour is very complex. With these sizes, the number of created phlogopite volume nuclei reaches an amount which enables the formation a significant amount of phlogopite phase. Consequently, a higher crystallization peak appears at lower temperature when all three crystal phases are formed and the resistance of the glass to crystallization abruptly decreases. Apart from this, the number of surface nuclei with these particle sizes still enables the separate formation of leucite and diopside phases, as can be

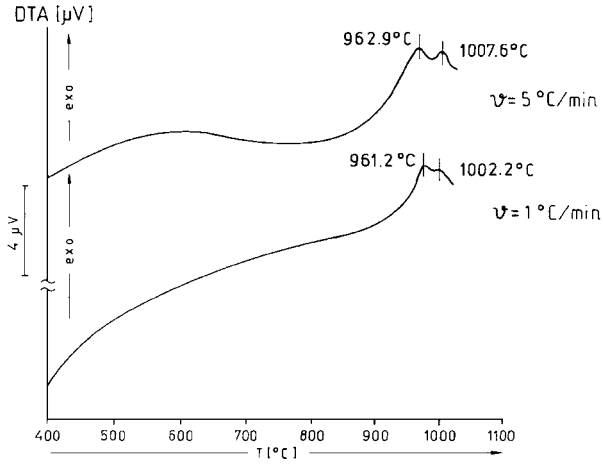

Figure 4 DTA traces recorded for power sample of particle size 0.1–0.2 mm, at heating rates 1°C/min and 5°C/min.

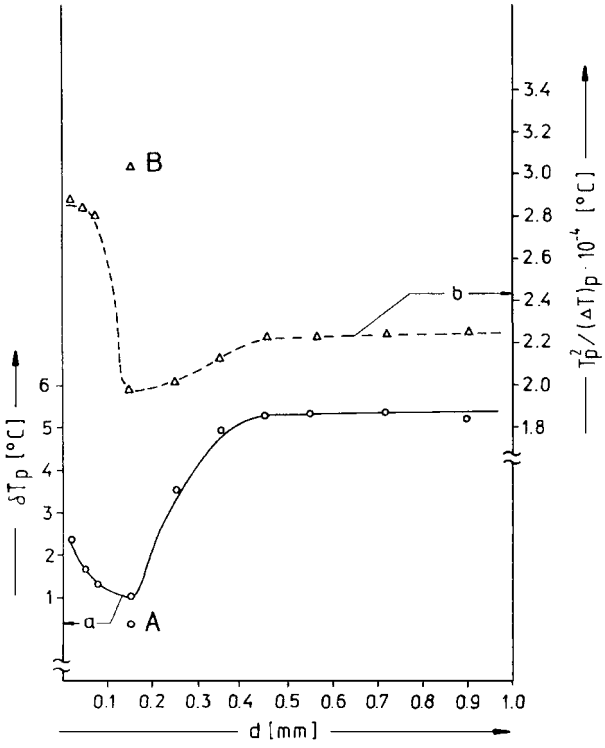

Figure 5 $(\delta T)_p$ and $T_p^2/(\Delta T)_p$ as a function of particle size.

judged by the appearance of the lower crystallization peak at a higher temperature. This is also indicated by the DTA curve of this sample recorded at the lower heating rate of 1°C/min (Fig. 4). For samples of larger particle sizes in the range of 0.2–1 mm, the surface-to-volume nuclei ratio decreases, which is accompanied by the formation of three crystal phases, the appearance of crystallization peaks in the lower temperature range of 960–980°C (Fig. 2, curve 2).

The relationship between δT_p, $T_p^2/(\Delta T)_p$ and the average particle size is presented in Fig. 5. As can be seen from this figure, complex curves of similar shape with three distinguishable regions were obtained. For average particles size <0.15 mm, the value of $T_p^2/(\Delta T)_p$ is in the range of $(2.81–2.88) \times 10^4$°C. Taking into account experimental error, the value $T_p^2/(\Delta T)_p$ can be regarded constant, which is in agreement with Equation 1. The value of δT_p decreases in this region. For particle sizes of about 0.15 mm, the situation is complex because of the existence of two exothermic peaks and change in the phase composition. In the curves, *a* and *b* used the higher peak at $T_{p1} = 962.9$°C (three phases). The value of both parameters for the lower peak at $T_{p2} = 1007.6$°C (two phases) is shown as the points A and B. In the region of 0.15–0.45 mm, both parameters reach minimums, extending to the point where the curves nearly reach their asymptotic values. For average particle sizes of >0.45 mm, both parameters have constant values.

Such a behaviour of δT_p and $T_p^2/(\Delta T)_p$ is in accordance with theoretical considerations for glasses the surface crystallization of which is being substituted by volume crystallization [13], without a change of the phase composition. These results point to the conclusion that the change of the phase composition during the substitution of the surface crystallization mechanism by the volume one has no effect on the parameters δT_p and $T_p^2/(\Delta T)_p$. Their behaviour depends only on the change of the surface-to-volume nuclei ratio.

3.3. Nucleation behaviour

The nucleation phenomenon was investigated by the method based on DTA measurements, proposed by Marotte *et al.* [11] and Ray *et al.* [14]. For this method, the following conditions should be satisfied: (a) nuclei should not be formed during nonisothermal heating in the DTA experiment and (b) bulk nucleation should occur in the glass. Previous investigations of nucleation in glass showed that it occurs at temperatures close to the glass transformation temperature (T_g) [2]. Dilatometric measurement of the investigated glass samples showed that its transformation occurs at $T_g = 658$°C. Investigations described in Section 3.4 show that crystallization of this glass is well manifested at temperatures $T > 850$°C. These results suggest that nucleation and crystal growth in this glass proceed in different temperature intervals, this enabling, by the selection of an appropriate heating rate for the DTA experiments, condition (a) to be satisfied. In our investigations, a heating rate $v = 7.5$°C/min was selected. The results presented in Section 3.2 show that in powder samples whose average particle sizes were >0.45 mm, volume crystallization is dominant. Accordingly, for the investigation of nucleation behaviour, powder glass a granulation of 0.5–0.63 mm was selected. Theoretical considerations [15, 16] applied to these experimental conditions also showed that a linear relationship between the logarithm of the number of nuclei per unit volume N and the reciprocal value of the crystallization peak temperature, $(1/T)$ exists:

$$\ln(N) = \frac{E_a}{RT_p} + \ln v + \text{const}, \qquad (2)$$

where v is the heating rate. According to Equation 2, an increase of the nuclei concentration causes a shift of the crystallization peak towards lower temperatures and *vice versa*. This enables a curve showing the relationship between $1/T_p$ and nucleation temperature T (similar to the nucleation rate curve), to be obtained.

This curve can be used to determine the temperature of the maximum nucleation rate, T_n.

The dependence of $1/T_p$ on T for this glass is presented in Fig. 6. It can be seen that in the temperature range $T = 600$–710°C, two asymetric maximums, positioned at the temperatures of 655°C and 675°C, are present. The maximum at 655°C is sharp and well expressed, while in the vicinity of the other maximum at 675°C, $1/T_p$ is nearly constant between the temperatures $T = 670^\circ$C and $T = 680^\circ$C. If the temperatures $T_{n1} = 655^\circ$C and $T_{n2} = 675^\circ$C are the temperatures of two maximum nucleation rates, then the character of this process can be analyzed: (I) from the relationship between these temperatures and the transformation temperature, T_g and (II) from the form of this curve. Comparing T_{n1} and T_{n2} with the transformation temperature, T_g, it can be noticed that T_{n2} satisfies the condition that $T_n \geq T_g$, which indicates that the glass nucleation is homogeneous [2]. The results presented in Section 3.4 show that $T_{n2} = 675^\circ$C corresponds to the temperature of the maximum nucleation rate of leucite, therefore, its nucleation can be regarded as being homogeneous. The situation with T_{n1} is more complex because it is very close to the T_g temperature. By taking into account experimental error, T_{n1} can satisfy this condition. The sole fact that $T_n \approx T_g$ is insufficient to prove that the nucleation is homogeneous, because many ineffective nucleating impurities can also produce a similar result [17]. If $T_{n1} < T_g$, then heterogeneous nucleation occurs [2]. In this case, nucleation in this glass is a combination of homogenous and heterogeneous. The same conclusion can be derived from the form of the curve presented in Fig. 6. This curve is similar to the curve for combined nucleation [17]. The results of XRD analysis helped resolve this problem (Section 3.4). These results show that T_{n1} corresponds to the temperature of the maximum nucleation rate of phlogopite. In addition, previous investigations of crystallization in alumosilicate glasses which contained fluoride and magnesia show

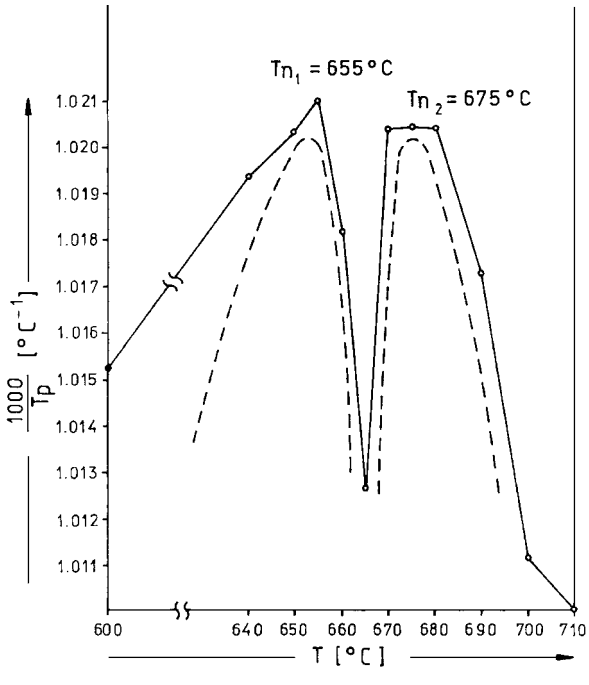

Figure 6 $1/T_p$ as a function of nucleating temperature.

that CaF_2 is segregated first if the content of MgO is low and mica type silicate are segregated first if the content of F^- anions is >1 wt% and the MgO content is >5 wt% [18]. Since the results of the chemical analysis (Section 3.1) show that the F^- anion content in this glass exceeds 1 wt% and the MgO content exceeds 5 wt%, then the phase separation occurs first at $T_{n1} = 655^\circ$C during heat treatment, (Section 3.6). One of these phases, being similar in composition to phlogopite, enables phlogopite crystals to develop on it at a later stage. It can be concluded that the nucleation proceeding at $T_{n1} = 655^\circ$C is homogeneous.

The results of XRD analysis (Section 3.4) also show that the volume ratio of the formed diopside phase is significant, but the temperature of its maximum nucleation rate is not visible in Fig. 6. A probable explanation for the absence of a maximum corresponding to the nucleation of this phase is that the number of diopside crystals is small, so their presence could not be identified during the DTA experiment. This small number of diopside crystals can be caused by: (I) a significant nucleation induction time, or (II) a low nucleation rate of diopside in the temperature range $T = 610$–710°C. The fact that T_{n1} and T_{n2} satisfy the condition that $T_n \geq T_g$, indicates that this glass is characterized by a short nucleation induction time. Therefore, it is quite probable that the nucleation rate of diopside in this temperature range is low. This is also indicated by the results obtained for a glass of similar chemical composition where the diopside nucleation temperature could also not be identified [4].

3.4. Crystallization of bulk glass

The results of XRD analysis of crystallized bulk samples are presented in Tables I and II as well as in Fig. 7. It can be seen from Table I, that crystalline phases were not observed in the samples heat treated at the nucleation temperatures (T_{n1} and T_{n2}). During a twostage heat treatment at the crystallization temperature $T_c = 870^\circ$C, the phlogopite phase crystallized alone. Only the phlogopite phase was formed in a glass sample treated at a crystallization temperature $T_c = 900^\circ$C when the annealing time was up to 180 min. With longer annealing times the diopside phase was also formed, regardless of the temperature of nucleation. During heat treatment at the nucleation temperature T_{n2} and crystallization temperature $T_c = 950^\circ$C for $t = 15$ min, only the phlogopite phase was formed. If the annealing time is 30 min or more, besides the diopside phase the leucite phase was also formed. However, in the sample nucleated at T_{n1} and crystallized at the same temperature for $t = 30$ min, no leucite phase was formed. The samples nucleated at the temperature T_{n1} and crystallized at the temperatures $T_c = 970^\circ$C and $T_c = 1010^\circ$C also did not contain the leucite phase. The sample nucleated at T_{n2} and crystallized at $T = 1010^\circ$C for $t = 600$ min does not contain a glass phase, but contains leucite, phlogopite, diopside and traces of the crystoballite phase. The quantitative fractions of these phases present in the samples given in Table II and Fig. 7, were obtained from Rietveld analysis.The obtained results show, that this glass crystallizes into a

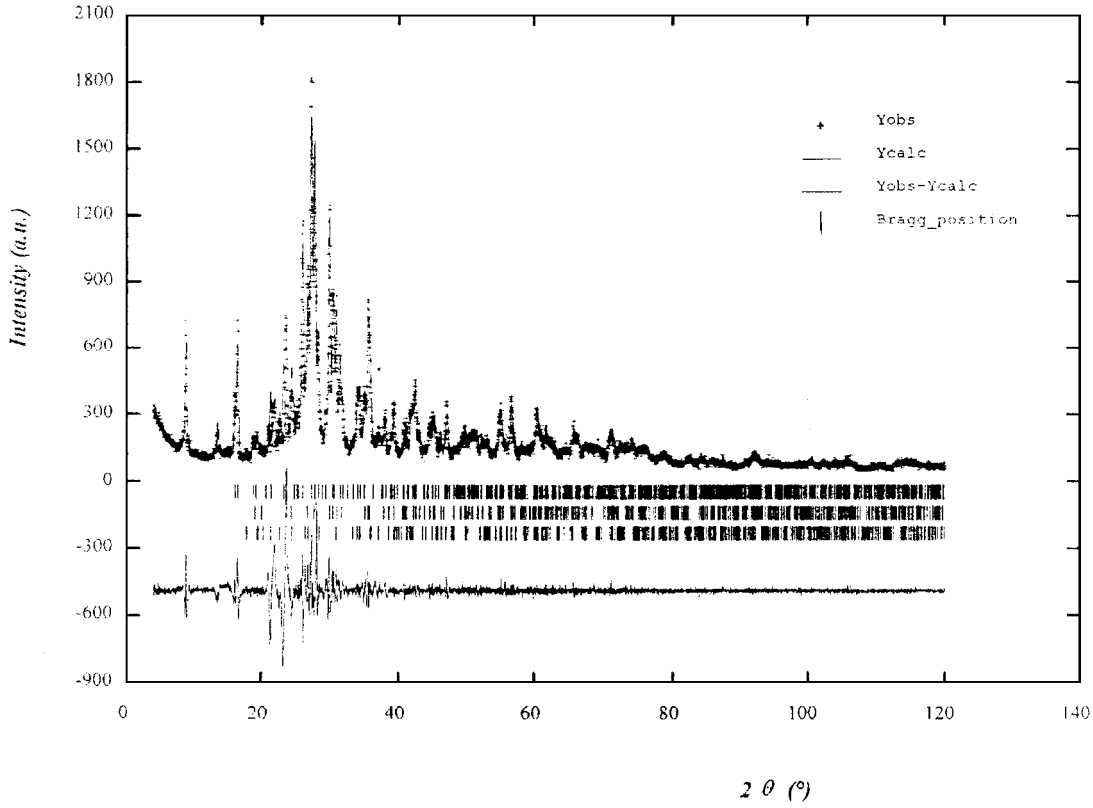

Figure 7 SEM micrographs for the sample heat treated at: (a) $T_{n1} = 675°C$ for $t = 600$ min and $T_c = 1100°C$ for $t = 600$ min, (b) $T_{n1} = 675°C$ for $t = 600$ min and $T_c = 870°C$ for $t = 450$ min and (c) $T_{n1} = 675°C$ for $t = 600$ min and $T_c = 1010°C$ for $t = 600$ min.

TABLE I Results of XRD analysis

T_n(°C)[a]	t_c(min)	Phase composition
655	600	G
675	600	G
	$T_c = 870°C$	
655	60	Ph + G
675	60	Ph + G
675	450	Ph + G
	$T_c = 900°C$	
655	15	Ph + G
655	30	Ph + G
655	60	Ph + G
655	180	Ph + D + G
655	600	Ph + D + G
675	180	Ph + D + G
	$T_c = 950°C$	
675	15	Ph + G
675	30	Ph + D + L + G
675	60	Ph + D + L + G
675	600	Ph + D + L + G
655	30	Ph + D + G
	$T_c = 970°C$	
655	180	Ph + D + G
	$T_c = 1010°C$	
655	180	Ph + D + G
675	600	Ph + D + L
	$T_c = 1100°C$	
675	600	Ph + D + L + G

[a]Nucleation time $t = 600$ min.
Ph-Phlogopite; D-Diopside; L-Leucite; G-Glass.

three component glass-ceramic, with the leucite phase dominating. The calculated unit cell dimensions were compared with literature data and no divergence was noticed. Moreover, the obtained cell dimensions for the phyllosilicate phase confirm the 1M-polytype fluorine-phlogopite phase.

These results also indicate the sequence of formation of the crystal phases during the isothermal heat treatment of bulk samples in the temperature range $T_c = 870$–$1100°C$. The sequence in which the phases begin to crystallize was: phlogopite, followed by diopside, and then by leucite. Such a sequence is an illustration of the influence of fluorine on the crystallization behaviour of this glass. The presence of fluorine in the glass structure enables the phlogopite ($KMg_3AlSi_3O_{10}F_2$) phase, in which it is present, to crystallize first throughout the whole temperature range. In this phase, TO_4 (T = Si, Al) tetrahedrons are arranged in layers, with three oxygen atoms participating in the formation of bridges. Since the experiments were performed in a two-stage regime, the growth of the crystal phases proceeds with a constant number of nuclei. This is an indication that the crystal grow rate of phlogopite is higher in comparison with the other two phases, because phlogopite crystallizes first over the whole temperature range. From the remaining glass, with no fluorine anions remaining, the diopside ($CaMgSi_2O_6$) phase is formed, with chained SiO_4 tetrahedrons in which two oxygen atoms participate in the bridge formation. Finally, the leucite ($KAlSi_2O_6$) phase is formed, with spatially arranged TO_4 tetrahedrons, in which four oxygen atoms participate in the bridge formation. It follows, that the crystal growth rate of the leucite phase is the lowest.

3.5. Crystallization kinetics

The results presented in Sections 3.3 and 3.4 show that the temperature of nucleation and crystal growth differ

TABLE II The most important crystallographic parameters for crystalline phases, obtained from Rietveld refinement of XRD pattern

Phase	Unit cell dimensions				Reliability factors		Quantitative volume fraction (%)
	a_o(Å)	b_o(Å)	c_o(Å)	β(°)	R_b(%)	R_f(%)	
Leucite	13.0778(4)	13.0778(4)	13.7077(4)	90.0	2.59	0.99	49
Diopside	9.7314(3)	8.9055(3)	5.2531(2)	105.969(2)	1.26	1.04	29
Phlogopite	5.3191(2)	9.1860(4)	10.1374(4)	99.886(4)	2.01	0.89	22

significantly (~150°C). For this reason, the selection of low heating rates enables the crystallization process to proceed at a constant number of nuclei. In this way, it is possible to neglect a complicated temperature dependence of the nucleation rate [13], which simplifies the problem and reduces it to the temperature dependencies of the crystal growth rates.

Non-isothermal methods, requiring small sample masses, are relatively easy to perform. However, the majority of the analytical methods for the quantitative analysis of non-isothermal data have been criticized for assuming the Arrhenian temperature dependence of the transformaton kinetics, and so do not have general validity [19–21]. This makes the calculated kinetic parameters reliable and unambiguous only in certain controlled cases. If the chemical composition of the melt and the crystal are the same, the growth rate is controlled by interface reactions. In this case, the Kissinger method is most often used for data analysis. A modified form of the Kissinger equations is as follows [22].

$$\ln\left(\frac{v^n}{T_p^2}\right) = -\frac{mE_a}{RT_p} + \text{const}, \qquad (3)$$

where m denotes the dimensionality of crystal growth. The values of the parameters n and m depend on the crystallization mechanism. The E_a values are calculated from the $\ln(v^n/T_p^2)$ versus $1/T_p$ dependence, using the appropriate values on n and m. It is believed that the so obtained E_a value has little physical significance in transformations where nucleation and crystal growth proceed simultaneously. However, if the glass sample is saturated with nuclei prior to crystal growth, this parameter can be interpreted as the activation energy of crystal growth [20, 23].

If the chemical compositions of the melt and crystal are different, both interdiffusion and the interface reactions can control crystal growth. For data analyses in diffusion controlled crystal growth, Equation 3 can also be used, but only the values of n and m exponents are different [24].

Microstructural investigations (Section 3.6) show that the leucite crystals grow in the form of two-dimensional dendrites. Such a morphology indicates layered, diffusion controlled kinetics of crystal growth. The phlogopite and diopside crystals grow in the form of spherulites. Such a morphology is associated with continuous, interface controlled kinetics of crystal growth. Growth kinetics, controlled by interface reactions, an associated with rearrangement of the network topology occurring at the crystal-melt interface, while

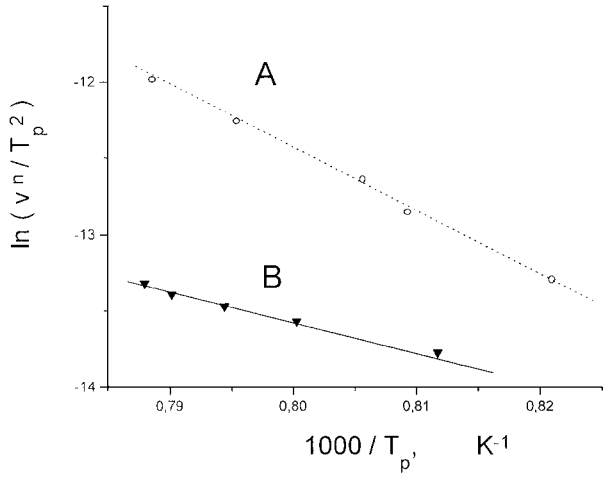

Figure 8 Rietveld refinement plot of glass sample heat treated at: $T_{n2} = 675$°C for $t = 600$ min and $T_c = 1010$°C for $t = 600$ min.

kinetics controlled by transfer processes an associated with interdiffusion, involving mobility of all the species present, since in the crystallization of viscous melts convection is nearly absent. As the interface processes and transport process are in series, the total transformation kinetics will be primarily controlled by the slower process. The analysis presented in Section 3.4 shows that in this case, leucite crystals grow at the slowest rate. Since the experiments were carried out with a constant number of nuclei, the problem of the stochastic nature of cluster evolution is avoided, leaving only diffusion controlled crystal growth. In this case, the temperature dependence of crystal growth is decisively influenced by the interdiffusion coefficient. Within the limited, narrow temperature range encompassing the crystallization peaks observed in the DTA experiments, it is reasonable to take the temperature dependence of the interdiffusion coefficients as Arrhenian. In accordance with the results presented in the Sections 3.2, 3.3 and 3.4, for the analyses of the crystallization kinetics, glass powder of the granulation 0.5–0.63 mm and heating rates of 2.5 to 10°C/min were selected. In order to ensure a condition of a constant number of nuclei, the glass powder sample of the smallest particle size (<0.038 mm) was selected, with surface nuclei dominating in number over the volume nuclei, formed during the DTA experiment. The T_p temperatures, recorded for both specimens at different heating rates, are presented in Table III. For two-dimensional crystal growth, $n = m = 1$, i.e. Equation 3 becomes equal to the Kissinger one. Using the Kissinger equation for the sample of granulation 0.5–0.63 mm, the value of the activation energy of crystal growth, $E_{aA} = 337 \pm 13$ kJ/mol (Fig. 8, line A) was

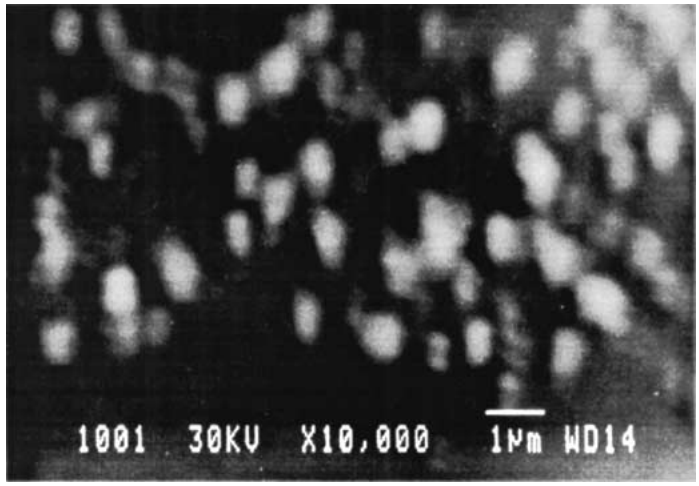

(a)

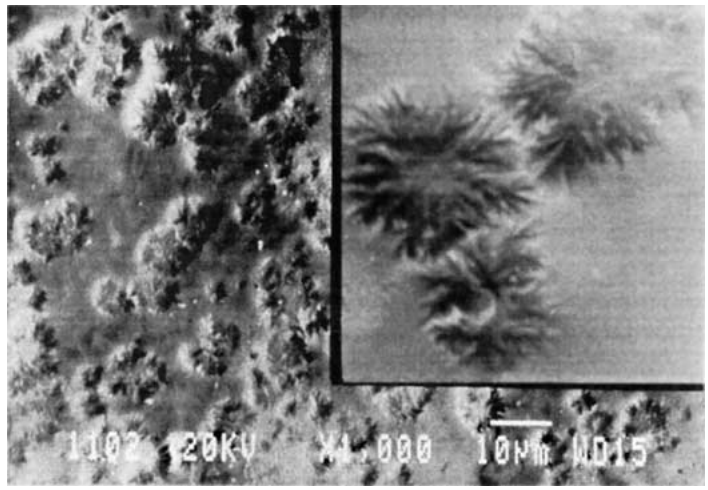

(b)

(c)

Figure 9 SEM micrographs for glass sample heat treated at: (a) $T_{n1} = 655^{\circ}$C for $t = 600$ min, (b) $T_{n1} = 655^{\circ}$C for $t = 600$ min and $T_c = 870^{\circ}$C for $t = 60$ min and (c) $T_{n1} = 655^{\circ}$C for $t = 600$ min and $T_c = 900^{\circ}$C for $t = 15$ min.

calculated. During surface crystallization and diffusion controlled growth, the value of the Avrami parameter is $n = 1/2$. With this value of n, the value of the activation energy of crystal growth for the specimen of granulation <0.038 mm, $E_{aB} = 309 \pm 16$ kJ/mol (Fig. 8, line B) was calculated. These results indicate that the E_a values for both specimens are, within the limits of experimental error, the same, so the mean value $E_a = 323 \pm 15$ kJ/mol was chosen for further consideration. The calculated E_a values also show that the activation energy of crystal growth of this glass is independent on the particle size, i.e. on the crystallization mechanism. By comparing this E_a value with the activation energy of the leucite crystal growth, $E_a = 319$ kJ/mol, obtained for a glass of similar composition [4], it can be seen that they are in good agreement.

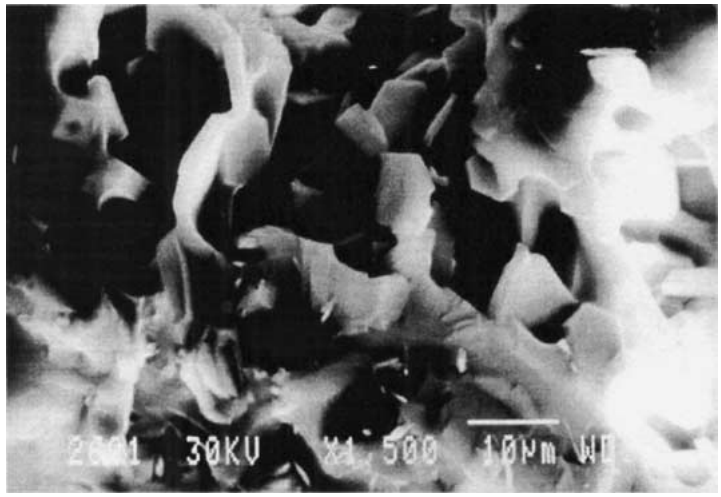

(a)

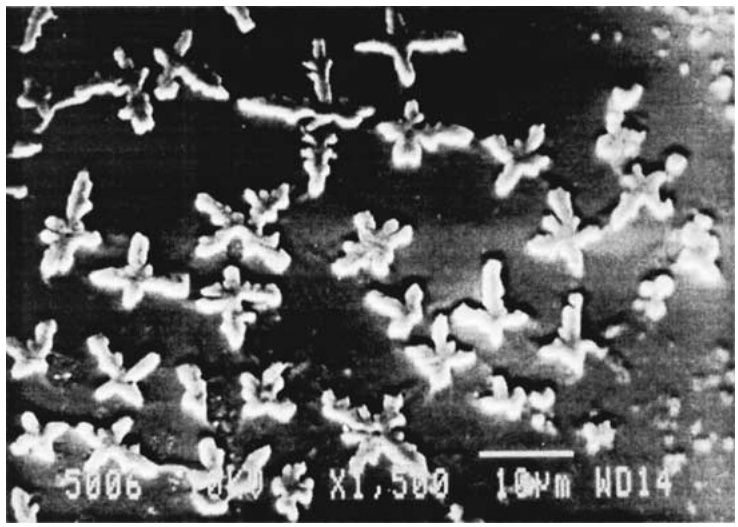

(b)

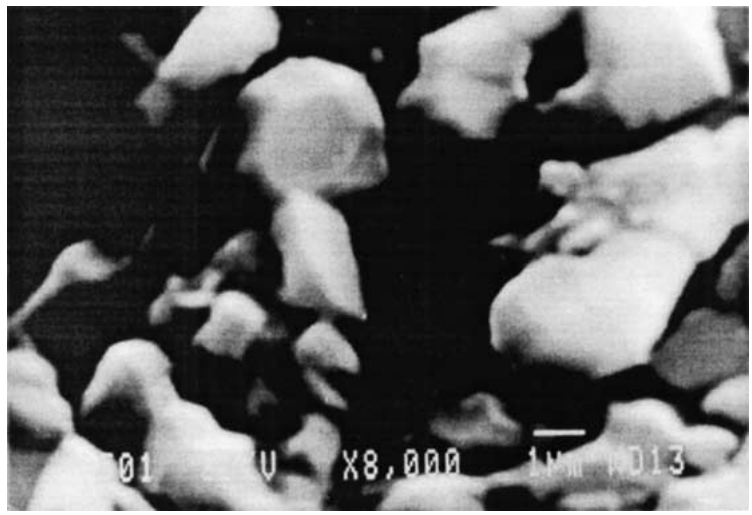

(c)

Figure 10 The plot of In (V^n/T_p^2) versus $1/T_p$ for powder samples particle size: (A) 0.5–0.63 mm, $n = 1$, (B) <0.038 mm, $n = 0.5$.

The value of the E_a should also agree with the activation energy of diffusion of the network-forming species in this glass. The mobility of the network-forming species controls the kinetics of phenomena such as glass crystallization [25]. However, the diffusion data for this composition of glass are not available. Studies of oxygen diffusion in multicomponent silicate glasses, in the temperature range above the glass transformation, showed that the activation energies of oxygen diffusion are in the range 200–250 kJ/mol [25, 26]. By comparing the obtained value, for crystal growth $E_a = 323$ kJ/mol, with these values, it is evident that they are in disagreement. This difference can, in part, be attributed to non-Arrhenian behaviour. Yet, such a difference indicates

TABLE III Shifting of crystallization peaks with change of the heating rates for powdered glass particle sizes <0.038 and 0.5–0.63 mm

Heating rate (°C/min)	Particle size <0.038 mm T_p(°C)	Particle size 0.5–0.63 mm T_p(°C)
2.5	958.8	944.8
4	976.4	962.4
5	985.6	968
6	992.4	–
7	995.9	–
7,5	–	984
10	–	994

that the diffusion units during oxygen diffusion are different to these involved during leucite crystal growth. This can be explained as being due to a complex interdiffusion mechanism in liquid silicates, where oxygen diffusion units of different mobilities exist.

The value of the parameter n can be determined from the same DTA curves by the Ozawa method [27]. This method avoids the assumption about a temperature dependence of the rate coefficient. For this reason, this analysis can provide a more reasonable assessment of the Avrami exponent [23]. The following relationship is used:

$$\frac{d\,(\log[\ln(1-x)]}{d\,\log v}|_T = -n \tag{4}$$

where x is the volume fraction crystallized in time t. The value of x is obtained from the relation $x = S/S_0$, where S denotes the peak surface at a selected temperature and S_0 is a total surface of the corresponding peak. The positions of the crystallization peaks on the DTA curves recorded for the specimen of granulation 0.5–0.63 mm, enable four values of x, at the temperature $T = 968$°C, to be obtained. A value of $n = 1.82 \pm 0.15$ was calculated, using Equation 4. In this case, the theoretical value of the Avrami parameter was $n = 1$. Taking into account experimental error, the value $n = 1.82$ is too high. This may be due to the influence of the nuclei which developed during glass quenching [23].

3.6. Microstructure

The evolution of the microstructure was investigated using bulk samples exposed to heat treatment under the conditions presented in Table I. For each sample, two micrographs were recorded: one of the surface and another of the interior (obtained by breaking the sample).

The micrograph of the interior of nucleated glass treated at $T_{n1} = 655$°C, is shown in Fig. 9a, in which a dropping region is clearly visible. The drops were about 0.5 μm large. This indicates that during heating under these conditions, phase separation precedes nucleation. The growth of phlogopite crystals can be seen on the sample annealed at $T_c = 870$°C, following nucleation at $T_{n1} = 655$°C (Fig. 9b). The XRD pattern for this sample, Table I, confirmed that a phlogopite phase had been formed. Phlogopite crystals in early stage development in the form of spherulites are visible on the outer side of the sample shown in Fig. 9b. Such a form of crystal growth, without manifested anisotropy, indicates continuous, interface controlled growth, proceeding on a nonfaceted, atomically rough interface [28]. Further growth of phlogopite crystals is detected in a sample annealed for a short period of time at $T_c = 900$°C, subsequent to nucleation at $T_{n1} = 655$°C. XRD analysis of this sample showed that only phlogopite phase was formed. The interior of the same sample is presented in Fig. 9c, from which it can be seen that the sample crystallized in characteristic folded and interstratified aggregates, with well developed single crystals occurring here and there.

Phlogopite crystal aggregates observed in the fissure of a sample annealed at $T_c = 1100$°C, following nucleation at $T_{n2} = 675$°C, are illustrated in Fig. 10a. The uniform size of the phlogopite crystals is obvious from this micrograph. A micrograph of a sample nucleated at $T_{n2} = 675$°C and annealed for some time at $T_c = 870$°C is presented in Fig. 10b. XRD analysis of this sample showed the formation of phlogopite phase. However, on the outer side of this sample, leucite dendrites in the early stage of development can be seen. Their expressed anisotropy along the ⟨001⟩ directions indicates a layered, diffusion controlled growth, proceeding on a faceted, atomically smooth interface [29]. A micrograph of a sample nucleated at $T_{n2} = 675$°C and subsequently annealed at $T_c = 1010$°C is presented in Fig. 10c. XRD analysis of this sample showed that it contained leucite, diopside and phlogopite phases. On the outer side of this sample, isometric crystals of well developed cubic form, typical of leuctite, are visible. However, smaller crystal grains with a prysmatic habit can also be seen on this micrograph. These grains probably represent the diopside phase.

4. Conclusion

In this study, the crystallization of a multicomponent glass containing F^- anions in the amount of 1.63 wt% was investigated. The results show that the crystallization of powder and bulk glass is very different. With particle size <0.15 mm, surface crystallization, accompanied by the formation of leucite and diopside phases, is dominant. With particle size about 0.15 mm, there phase (phlogopite, diopside and leucite), are formed, accompanied by an abrupt decrease in the resistance of the glass to crystallization. With particle size in the range 0.15 to 0.45 mm, both surface and volume crystallization are significant, while with particle size >0.45 mm, volume crystallization is dominant.

Investigations of the nucleation process in the temperature range of 600–710°C, showed the existence two of nucleation temperatures, $T_{n1} = 655$°C and $T_{n2} = 675$°C. The temperature $T_{n1} = 655$°C corresponds to the maximum nucleation rate of the phlogopite phase. $T_{n2} = 675$°C corresponds to maximum nucleation rate of the leucite phase. Relative to the transformation temperature, T_g, these temperatures satisfy the condition that $T_{n1,2} \geq T_g$.

The results of the investigation of the crystallization of bulk glass show that at a temperature of $T_c = 870$°C, only a phlogopite phase is formed. At a crystallization temperature of $T_c = 900$°C, in addition to phologopite, a diopside phase is formed. At a crystallization temperature of $T_c = 950$°C, in addition to phlogopite and diopside, a leucite phase is also formed. The sample

crystallized at $T_c = 1010°C$ does not contain a glassy phase. Quantitative analysis of this sample showed that it contained 49% leucite, 29% diopside and 22% phlogopite. The dimensions of the unit cells were compared to the literature data and no significant divergence was noticed.

Analyses of the crystallization kinetics showed that in this glass the crystallization process is controlled by leucite formation. An activation energy of leucite crystal growth of $E_a = 323 \pm 15$ kJ/mol and an Avrami parameter of $n = 1.82$ were determined.

An investigation of the microstructure showed that the leucite crystals grow in the form of two-dimensional dendrites, with well manifested anisotropy. Such a morphology is an indication of layered, diffusion controlled growth, proceeding on an atomically smooth faceted crystal/glass interface. The phlogopite crystals grow in the form of spherulites. Such a morphology is an indication of continuous, interface controlled growth, proceeding on an atomically rough, nonfaceted crystal/glass interface.

References

1. P. F. JAMES, B. SCOTT and P. AMSTRONG, *Physics Chem. Glasses* **19** (1978) 24.
2. E. D. ZANOTTO and M. C. WEINBERG, *ibid.* **30** (1989) 186.
3. W. VOGEL, "Glaschemie," 2nd ed (VEB, Leipzig, 1983).
4. M. B. TOŠIĆ, M. M. MITROVIĆ and R. Ž. DIMITRIJEVIĆ, *J. Mater. Sci.* **35** (2000) 3659.
5. D. C. PALMER, E. K. H. SALJE and W. W. SCHMAL, *Phys. Chem. Minerals* **16** (1989) 714.
6. W. HOLAND, M. FRANK and V. RHEINBERGER, *J. Non-Cryst. Solids* **180** (1995) 292.
7. H. M. RIETVELD, *J. Appl. Cryst.* **2** (1969) 65.
8. J. RODRIGUEZ-CARVAJAL, in The XV Congress of the IUCR, Toluse 1990 France, Book of Abstract, p. 127.
9. C. S. RAY and D. E. DAY, *Thermochim. Acta* **280/281** (1996) 163.
10. C. S. RAY, Q. YANG, W. HAUNG and D. E. DAY, *J. Amer. Ceram. Soc.* **79** (1996) 3155.
11. A. MAROTTA, A. BURI and F. BRANDA, *J. Mater. Sci.* **16** (1981) 341.
12. J. A. AUGIS and J. E. BENNETT, *J. Thermal. Anal.* **13** (1978) 283.
13. K. F. KELTON, K. LAKASHMI NARAYAN, L. F. LEVINE, T. C. CULL and C. S. RAY, *J. Non-Cryst. Solids* **204** (1996) 13.
14. C. S. RAY and D. E. DAY, *J. Amer. Ceram. Soc.* **73** (1990) 439.
15. M. C. WEINBERG, *ibid.* **74** (1991) 1905.
16. K. F. KELTON, *ibid.* **75** (1992) 2449.
17. M. C. WEINBERG, *ibid.* **70** (1987) 475.
18. S. LYNG, J. MARKALI, J. KROGH-MOE and N. H. LUNDBERG, *Physics Chem. Glasses* **11** (1970) 6.
19. H. YINNON and D. R. UHLMANN, *J. Non-Cryst. Solids* **54** (1983) 253.
20. M. C. WEINBERG, *ibid.* **127** (1991) 151.
21. K. F. KELTON, *ibid.* **163** (1993) 283.
22. K. MATUSITA and S. SAKA, *Phys. Chem. Glasses* **20** (1979) 81.
23. K. F. KELTON, *Mater. Sic. Eng.* A **226–228** (1997) 142.
24. D. R. MACFARLANE, M. MATECKI and M. POULAIN, *J. Non-Cryst. Solids* **64** (1984) 351.
25. H. A. SCHAEFFER, *ibid.* **67** (1984) 19.
26. H. YINNON and A. R. COOPER, *Phys. Chem. Glasses* **21** (1980) 204.
27. T. OZAWA, *Polymer* **12** (1971) 150.
28. G. H. BEALL, *J. Non-Cryst. Solids* **129** (1991) 163.
29. K. WATANABE, E. A. GIESS and M. W. SHAFER, *J. Mater. Sic.* **20** (1985) 508.

Received 29 June 2001
and accepted 30 January 2002